JOURNAL OF CHEMICAL & ENGINEERING DATA

ARTICLE

pubs.acs.org/jced

Liquid−Liquid Equilibria for {1-Ethyl-3-methylimidazolium Diethylphosphate or 1-Ethyl-3-methylimidazolium Ethylsulfate} + 4,6-Dimethyldibenzothiophene + Dodecane Systems at 298.2 K and 313.2 K

Leonardo Hadlich de Oliveira[†] and Martín Aznar*

School of Chemical Engineering, University of Campinas, Av. Albert Einstein 500, 13083-852, Campinas-SP, Brazil

ABSTRACT: Liquid−liquid equilibrium (LLE) data for {1-ethyl-3-methylimidazolium diethylphosphate ([emim][DEtPO$_4$]) or 1-ethyl-3-methylimidazolium ethylsulfate ([emim][EtSO$_4$])} + 4,6-dimethyl-dibenzothiophene (4,6-DMDBT) + dodecane systems, at (298.2 and 313.2) K and atmospheric pressure (≈ 95 kPa), were determined by refractometry. 4,6-DMDBT is one of the most difficult diesel sulfur pollutants to remove by the conventional process of hydrodesulfurization (HDS). Extraction of 4,6-DMDBT from dodecane (used as model diesel oil) was analyzed in terms of solute distribution coefficient, solvent selectivity, and percent of extraction. The results indicate that [emim][DEtPO$_4$] is a better solvent for extractive desulfurization of dodecane than [emim][EtSO$_4$]. The Hand and Othmer−Tobias correlations, used to ascertain the quality of the experimental data, presented R^2 > 0.98 for systems with [emim][DEtPO$_4$] and R^2 > 0.96 for systems with [emim][EtSO$_4$]. The nonrandom two-liquid (NRTL) model was used to correlate the LLE data and showed root-mean-square deviations between experimental and calculated mole fractions ≤ 0.0002.

INTRODUCTION

The sulfur compounds present in fossil fuels cause pollution by vehicle and industrial SO_X emissions. Moreover, the sulfur inhibits vehicle control pollution equipment performance.[1] For this reason, the maximum mass fraction of sulfur (w) in diesel oil was fixed, by legislation, to $w = 1.0 \cdot 10^{-5}$ in Japan and the European Union, $1.5 \cdot 10^{-5}$ in the United States, and $5.0 \cdot 10^{-5}$ in Brazil.[2]

The usual process of hydrodesulfurization (HDS) requires severe operational conditions (> 573.15 K, > 30 bar, large amounts of H_2, expensive catalysts, etc.)[3] to achieve sulfur mass fractions below $5.0 \cdot 10^{-5}$,[4] but it is not effective to remove some sulfur compounds, such as the sterically hindered dibenzothiophene (DBT) and its derivatives, 4-methyldibenzothiophene (4-MDBT) and 4,6-dimethyldibenzothiophene (4,6-DMDBT);[5] for this reason, other processes to achieve the deep desulfurization of diesel oil, such as biodesulfurization (BDS), oxidesulfurization (ODS), and extractive desulfurization (EDS) with ionic liquids, have received attention in recent years.

In literature, the removal of 4,6-DMDBT is reported for model[6−13] and real[14−20] diesel oil. Also, some works show data for the extractive desulfurization of DBT and 4-MDBT with ionic liquids,[3,21,22] and others show liquid−liquid equilibrium (LLE) data for alkane + thiophene + ionic liquid systems.[23−28] In a recent paper[27] the authors reported LLE data for the extraction of 4-MDBT from dodecane.

Since there is no report of phase equilibrium data involving the systems studied here, LLE data were obtained for the systems {1-ethyl-3-methylimidazolium diethylphosphate ([emim][DEtPO$_4$]) or 1-ethyl-3-methylimidazolium ethylsulfate ([emim][EtSO$_4$])} + 4,6-DMDBT + dodecane as model diesel oil, at 298.2 K and 313.2 K and atmospheric pressure (≈ 95 kPa).

EXPERIMENTAL METHODS

Chemicals. The properties of the used chemicals are listed in Table 1. This work reports the refractive index (n_D) of [emim][DEtPO$_4$] at (298.2 and 313.2) K and [emim][EtSO$_4$] at 313.2 K, not yet available in literature; n_D of [emim][EtSO$_4$] at 313.2 K and dodecane at 298.2 K were determined by Alonso et al.,[26] while Wohlfarth[28] reports n_D for dodecane at 313.2 K.

Purification. For the removal of residual volatile compounds and moisture from the ionic liquids, approximately 50 g of each ionic liquid was inserted in a sealed glass flask to avoid contact with air and subjected to vacuum (8 kPa) and magnetic stirring at 323.15 K for 24 h. After that, the ionic liquids were stored under nitrogen atmosphere, and their water mass fraction was measured by Karl Fischer titration (Metler Toledo DL31 Karl Fischer titrator), giving values below $5.0 \cdot 10^{-4}$ for both ionic liquids. Other chemicals were used as received.

Procedure. Experiments were carried out in equilibrium cells, such as suggested by Sandler[29] and described elsewhere.[30] The cell temperature was regulated by a Tecnal TE-184 thermostatic bath (± 0.1 K).

The cloud point method, similar to that of Letcher and Siswana,[31] was utilized for determination of binodal curves in the ionic liquid-rich phase, by dropwise adding dodecane to known binary homogeneous mixtures of 4,6-DMDBT + ionic liquid using a syringe, until constant turbidity (saturation). Then, the refractive index of the mixture was measured, in triplicate, with a Mettler-Toledo RE 40D refractometer, to build calibration curves (n_D as function of composition) on the

Received: October 12, 2010
Accepted: March 22, 2011
Published: April 02, 2011

Table 1. Properties of the Pure Components[a]

chemical	M	n_D 298.2 K		n_D 313.2 K		mass percent purity	supplier
	g·mol^{-1}	exp	lit.	exp	lit.		
[emim][DEtPO$_4$]	264.26	1.4733	NA	1.4691	NA	≥ 0.98	Aldrich
[emim][EtSO$_4$]	236.29	1.4789	1.47903[26]	1.4745	NA	0.95	Fluka
4,6-DMDBT	212.31	-	-	-	-	0.97	Aldrich
dodecane	170.33	1.4196	1.42011[26]	1.4131	1.4129[28]	0.996	Fluka

[a] NA: not available; ref 26, Alonso et al., 2008; ref 28 Wohlfarth, 2008.

binodal curve. The ionic liquid did not dissolve in the binary alkane-rich phase; this was concluded experimentally, adding a drop of ionic liquid to pure dodecane or to a binary {dodecane + 4,6-DMDBT} mixture, verifying no solubilization of the drop and no change in refractive index of the dodecane or the mixture. So, the calibration curves of alkane-rich phase were determined by measuring in triplicate the refractive index of known binary {dodecane + 4,6-DMDBT} mixtures.

In each LLE experiment, a ternary mixture of known composition within the immiscibility region was prepared by weighing the components directly inside the cell, using a Shimadzu AX200 analytical balance (± 0.0001 g). An approximate amount, between 8 g and 10 g of total mass, was utilized for each equilibrium experiment. After that, the mixture was vigorously agitated with a Fisatom 752 magnetic stirrer for 12 h, to allow a close contact between phases, and decanted for 24 h to equilibrium phases settle down. The system separate in two clean liquid phases. Also, the binary solid−liquid equilibrium (SLE) was determined for dodecane + 4,6-DMDBT to establish the maximum solubility of 4,6-DMDBT in dodecane. In SLE experiments, pure 4,6-DMDBT precipitates in equilibrium with a saturated mixture of dodecane + 4,6-DMDBT. So, in both LLE and SLE, the refractive index of liquid phase was measured in triplicate and the average used for composition determination.

For the [emim][EtSO$_4$] + 4,6-DMDBT + dodecane system at 298.2 K, the cloud point method was replaced by a graphical method, which consists in estimate graphically the composition of the ionic liquid-rich phase, knowing the composition of the alkane-rich phase and considering no loss of mass during weighing, agitation, and settling, that is, forcing the interception of tie lines through feed-point composition. This method was used because the level of confidence (mean value ± standard deviation) of the triplicate refractive index measurement of one cloud point matches the level of confidence of the next cloud points, even for a standard deviation ≤ 0.0001 for each triplicate refractive index.

THERMODYNAMIC MODELING

The LLE conditions are represented by equality of pressure, temperature, and component chemical potential between the two liquid phases. The LLE calculation is well-known and basically defined by:

$$x_i^{\mathrm{I}}\gamma_i^{\mathrm{I}} = x_i^{\mathrm{II}}\gamma_i^{\mathrm{II}} \qquad (1)$$

Table 2. Mass Fraction w, Refractive Indexes n_D, and Standard Deviations σ_p of Points on the Binodal Curve for Ionic Liquid (1) + 4,6-DMDBT (2) + Dodecane (3) at 298.2 K and 313.2 K

T/K	[emim][DEtPO$_4$] w_1	w_2	n_D	$10^4\sigma_p$	[emim][EtSO$_4$] w_1	w_2	n_D	$10^4\sigma_p$
298.2	0.9967	0.0000	1.4727	0.00	0.9983	0.0000	1.4788	0.00
	0.9957	0.0012	1.4731	0.00	0.9974	0.0002	1.4789	0.58
	0.9942	0.0025	1.4733	0.58	0.9971	0.0004	1.4789	0.00
	0.9921	0.0035	1.4735	0.58	0.9970	0.0006	1.4791	0.58
					0.9965	0.0010	1.4790	1.00
313.2	0.9951	0.0000	1.4685	0.58	0.9986	0.0000	1.4749	0.58
	0.9937	0.0008	1.4686	0.00	0.9961	0.0006	1.4750	0.58
	0.9902	0.0037	1.4691	0.00	0.9953	0.0014	1.4751	0.00
	0.9873	0.0045	1.4694	0.00	0.9945	0.0030	1.4754	0.00

where γ_i and x_i are the activity coefficient and mole fraction of component i, and superscripts I and II refer to the two liquid phases.

The nonrandom two-liquid model (NRTL)[32] was used for the calculation of activity coefficient and correlation of experimental LLE data with the estimation of new energy interaction parameters by using the Fortran code TML-LLE 2.0.[33] This procedure is based on the modified Simplex method[34] and consists of the minimization of a concentration-based objective function, F.[35] Calculated molar fractions were compared with those obtained experimentally through root-mean-square deviations, δx. The equations used for thermodynamic modeling were previously showed by Oliveira and Aznar.[27]

RESULTS AND DISCUSSION

Cloud Points and Calibration Curves. The mass fractions (w), refractive indexes, and standard deviations for refractive index measurements (σ_p) of the cloud points are shown in Table 2. σ was calculated by eq 2,

$$\sigma_p = \sqrt{\frac{\sum(n_{D,p} - \overline{n})^2}{(d-1)}} \qquad (2)$$

where d is the number of data points, $n_{D,p}$ is the refractive index of each data point p, and $\overline{n}$ is the refractive index average. The uncertainty of cloud point dodecane mole fraction is < 0.0008 for each cloud point for all systems.

dx.doi.org/10.1021/je100991y |J. Chem. Eng. Data 2011, 56, 2005–2012

The regression of data in Table 2 gave the equations of calibration curves for [emim][DEtPO$_4$] (1) + 4,6-DMDBT (2) + dodecane (3):

$$n_D(298.2\ K) = -37.615 + 78.785w_1 - 39.699{w_1}^2 \quad (3a)$$

$$n_D(298.2\ K) = 1.4728 + 0.2211w_2 \quad (3b)$$

$$n_D(313.2\ K) = 1.5880 - 0.1201w_1 \quad (4a)$$

$$n_D(313.2\ K) = 1.4685 + 0.044w_2 + 33.102{w_2}^2 \quad (4b)$$

Table 3. Mass Fractions w, Refractive Indexes n_D, and Standard Deviations σ_p of Binary Mixtures of Dodecane (1) + 4,6-DMDBT (2) at 298.2 K and 313.2 K

298.2 K			313.2 K		
w_2	n_D	$10^4\ \sigma_p$	w_2	n_D	$10^4\ \sigma_p$
0.0000	1.4196	0.00	0.0000	1.4131	0.00
0.0037	1.4201	0.00	0.0037	1.4137	0.00
0.0062	1.4206	0.58	0.0062	1.4141	0.00
0.0089	1.4210	0.00	0.0089	1.4146	0.00
0.0128[a]	**1.4216**	**0.00**	**0.0190**	**1.4163**	**0.00**

[a] SLE in bold: solid phase = pure 4,6-DMDBT.

and for [emim][EtSO$_4$] (1) + 4,6-DMDBT (2) + dodecane (3):

$$n_D(313.2\ K) = 1.4749 + 0.0005 \exp\left(\frac{w_1 - 0.9945}{0.00093}\right) \quad (5a)$$

$$n_D(313.2\ K) = 1.4749 + 0.1633w_2 \quad (5b)$$

Note that the equations for the system with [emim][EtSO$_4$] at 298.2 K were not obtained, because the composition of the ionic liquid-rich phase was determined by the graphical method.

The binary dodecane (1) + 4,6-DMDBT (2) calibration curve points are shown in Table 3. The values in bold are the SLE data. They represent the maximum solubility of 4,6-DMDBT in dodecane. An increase of 15 K rises 48 % solubility of 4,6-DMDBT in dodecane. Applying linear regression to data in Table 3, the equations obtained are:

$$n_D(298.2\ K) = 1.4196 + 0.1601w_2 \quad (6a)$$

$$n_D(313.2\ K) = 1.4131 + 0.1675w_2 \quad (6b)$$

eqs 3a to 6b quantify the ionic liquid and 4,6-DMDBT mole fractions. The dodecane mole fraction was calculated by applying mass balance.

Equilibrium Data. The LLE data (mole fractions) for the ternary systems {[emim][DEtPO$_4$] or [emim][EtSO$_4$]} + 4,6-DMDBT + dodecane at 298.2 K and 313.2 K and atmospheric pressure (≈ 95 kPa) are reported in Tables 4 and 5. Also, in these tables are the standard deviation for the refractive index (σ_p), the

Table 4. Liquid−Liquid Equilibrium Data for the [emim][DEtPO$_4$] (1) + 4,6-DMDBT (2) + Dodecane (3) System at 298.2 K and 313.2 K[a]

			LLE data[b]										
	feed		dodecane phase				ionic liquid phase						
T/K	x_1	x_2	x_1	x_2	n_D	$10^4\sigma_p$	x_1	x_2	n_D	$10^4\sigma_p$	K	S	10^4u
298.2	0.2647	0.0018	0	0.0024	1.4201	0.58	0.9936	0.0004	1.4729	0.58	0.1555	25.9	0.5
	0.2620	0.0036	0	0.0045	1.4205	0.00	0.9930	0.0011	1.4730	0.58	0.2488	42.4	0.1
	0.2581	0.0058	0	0.0065	1.4209	0.58	0.9925	0.0017	1.4731	0.58	0.2582	43.9	5.7
313.2	0.2767	0.0051	0	0.0062	1.4144	0.00	0.9903	0.0023	1.4687	0.58	0.3744	50.3	0.1
	0.2758	0.0074	0	0.0086	1.4149	0.58	0.9868	0.0041	1.4690	0.00	0.4704	51.3	0.4
	0.2765	0.0088	0	0.0101	1.4152	0.00	0.9833	0.0053	1.4693	0.58	0.5276	46.0	0.8

[a] Ionic liquid/dodecane feed mass ratio = 0.6. [b] Uncertainty in mole fractions < 0.0004.

Table 5. Liquid−Liquid Equilibrium Data for [emim][EtSO$_4$] (1) + 4,6-DMDBT (2) + Dodecane (3) System at 298.2 K and 313.2 K[a]

			LLE data[b]										
	feed		dodecane phase				ionic liquid phase						
T/K	x_1	x_2	x_1	x_2	n_D	$10^4\sigma_p$	x_1	x_2	n_D	$10^4\sigma_p$	K	S	10^4u
298.2	0.3023	0.0019	0	0.0027	1.4201	0.00	0.9967	0.0002			0.0569	18.1	
	0.2991	0.0041	0	0.0057	1.4207	0.00	0.9962	0.0005			0.0810	24.3	
	0.2976	0.0071	0	0.0097	1.4215	0.00	0.9961	0.0009			0.0917	29.8	
313.2	0.3010	0.0053	0	0.0072	1.4146	0.58	0.9948	0.0007	1.4750	0.58	0.0940	20.5	0.5
	0.3067	0.0082	0	0.0106	1.4153	1.00	0.9938	0.0014	1.4751	1.15	0.1283	26.4	4.6
	0.2964	0.0106	0	0.0135	1.4159	0.58	0.9936	0.0020	1.4752	0.58	0.1512	34.0	5.6

[a] Ionic liquid/dodecane feed mass ratio = 0.6. [b] Uncertainty in mole fractions < 0.0004 for 313.2 K and < 0.0003 for 298.2 K.

dx.doi.org/10.1021/je100991y |J. Chem. Eng. Data 2011, 56, 2005–2012

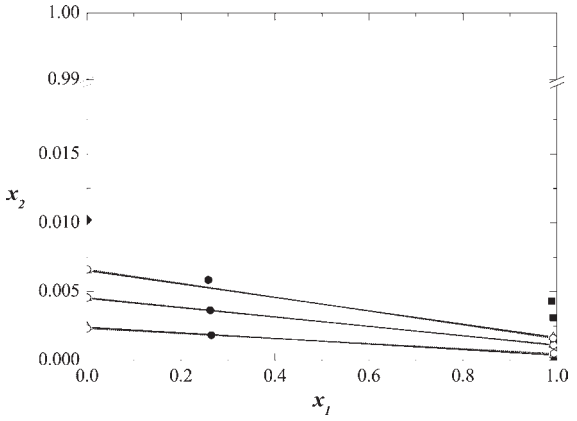

Figure 1. Experimental and calculated phase equilibrium data for the system [emim][$DEtPO_4$] (1) + 4,6-DMDBT (2) + dodecane (3) at 298.2 K: ■, cloud points; ●, feed points; (△, solid line), tie-lines; ♦, 4,6-DMDBT saturation in dodecane; (○, dotted line), NRTL correlation. Ionic liquid/dodecane feed mass ratio = 0.6.

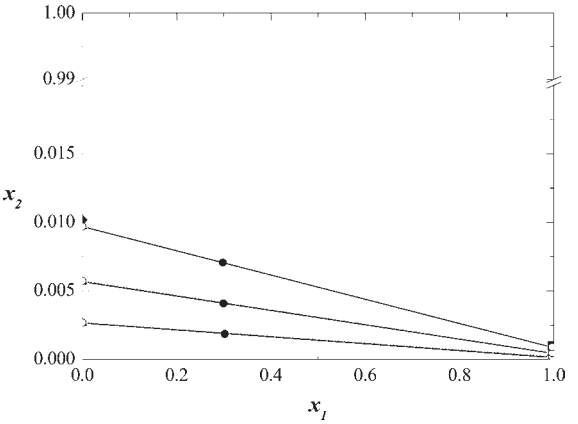

Figure 3. Experimental and calculated phase equilibrium data for the system [emim][$EtSO_4$] (1) + 4,6-DMDBT (2) + dodecane (3) at 298.2 K: ■, cloud points; ●, feed points; (△, solid line), tie-lines; ♦, 4,6-DMDBT saturation in dodecane; (○, dotted line), NRTL correlation. Ionic liquid/dodecane feed mass ratio = 0.6.

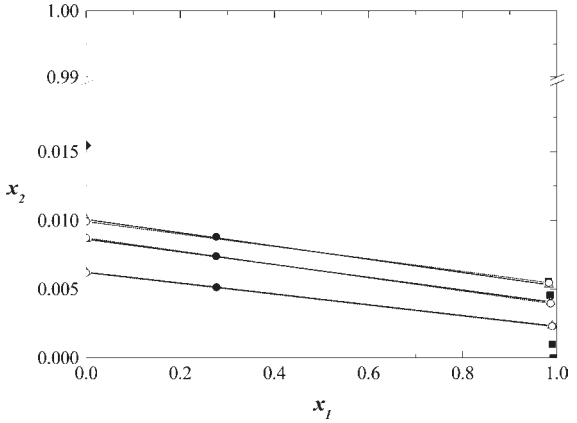

Figure 2. Experimental and calculated phase equilibrium data for the [emim][$DEtPO_4$] (1) + 4,6-DMDBT (2) + dodecane (3) system at 313.2 K: ■, cloud points; ●, feed points; (△, solid line), tie-lines; ♦, 4,6-DMDBT saturation in dodecane; (○, dotted line), NRTL correlation. Ionic liquid/dodecane feed mass ratio = 0.6.

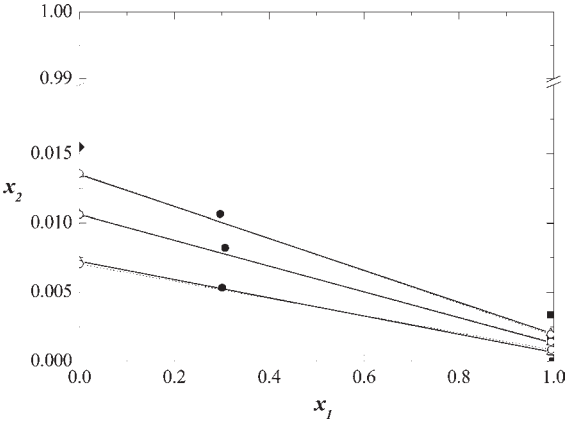

Figure 4. Experimental and calculated phase equilibrium data for the [emim][$EtSO_4$] (1) + 4,6-DMDBT (2) + dodecane (3) system at 313.2 K: ■, cloud points; ●, feed points; (△, solid line), tie-lines; ♦, 4,6-DMDBT saturation in dodecane; (○, dotted line), NRTL correlation. Ionic liquid/dodecane feed mass ratio = 0.6.

distribution coefficient (K), and the selectivity of the solvent (S) both given by Oliveira and Aznar.[27]

Rectangular diagrams representing the phase equilibrium data are shown in Figures 1 to 4. In these figures, it is observed that the LLE region is at the bottom of a conventional ternary diagram (not shown here), as noted by Esser et al.[3] The slope of the tie-lines, the distribution of 4,6-DMDBT in both phases (Figure 5), and selectivity values above 40 (Figure 6) lead to the conclusion that [emim][$DEtPO_4$] is a better solvent than [emim][$EtSO_4$] for the extraction of 4,6-DMDBT from dodecane at the two temperatures and that 4,6-DMDBT solubilizes preferably in dodecane phase.

The quality of the LLE data is pointed out by two tests:

(a) Using eq 7, which is the well-known linear algebra equation to calculate the distance (u) between a straight line and a point,[36] the distance between each tie line and the respective feed composition was calculated.

$$u = \frac{|ax_1^{\text{feed}} + bx_2^{\text{feed}} + c|}{\sqrt{a^2 + b^2}} \tag{7a}$$

$$a = x_2^{\text{ap}} - x_2^{\text{ilp}} \tag{7b}$$

$$b = x_1^{\text{ilp}} - x_1^{\text{ap}} \tag{7c}$$

$$c = x_1^{\text{ap}} x_2^{\text{ilp}} - x_1^{\text{ilp}} x_2^{\text{ap}} \tag{7d}$$

Superscripts feed, ap, and ilp refer to feed, alkane-rich phase, and ionic liquid-rich phase. Figure 7 shows the geometric scheme of the u calculation by eq 7. This calculation allows us to quantify the experimental error by analysis and loss of mass in both phases and feed. The values of u are shown in Tables 4 and 5. Tie lines are very close to the feed composition. An uncertainty of experimental mole fraction ≤ 0.0004 was obtained using the refractive index method. For systems with [emim][$EtSO_4$] at 298.2 K, tie lines were forced to pass through feed points, giving u = 0. So, the experimental mole fraction uncertainty for this system was considered only for

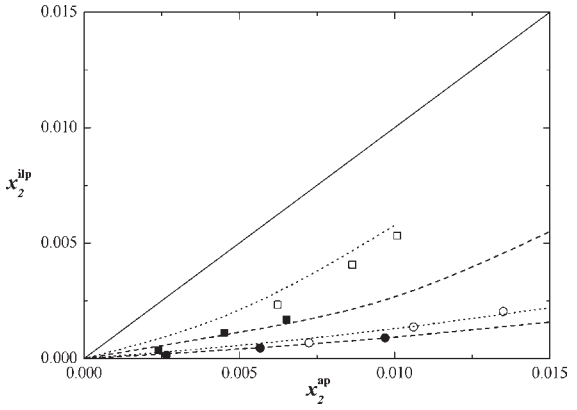

Figure 5. Distribution of 4,6-DMDBT between ionic liquid and dodecane rich phase: □, [emim][DEtPO$_4$]; ○, [emim][EtSO$_4$]; full symbols and dashed lines, 298.2 K; open symbols and dotted lines, 313.2 K; lines are calculated by NRTL. Ionic liquid/dodecane feed mass ratio = 0.6. Component numbers: ionic liquid (1), 4,6-DMDBT (2), dodecane (3).

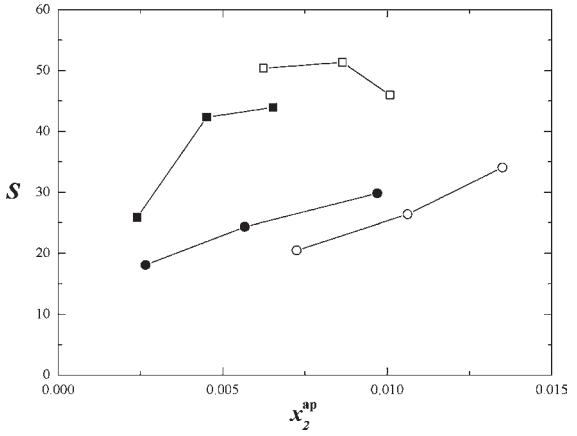

Figure 6. Selectivity S of ionic liquids for each mole fraction of 4,6-DMDBT after equilibrium in the alkane phase x_2^{ap}: □, [emim][DEtPO$_4$]; ○, [emim][EtSO$_4$]; full symbols, 298.2 K; open symbols, 313.2 K. Ionic liquid/dodecane feed mass ratio = 0.6. Component numbers: ionic liquid (1), 4,6-DMDBT (2), dodecane (3).

alkane-rich phase, which is ≤ 0.0003 and was obtained from the standard deviation of triplicate refractive index measurement for each tie line. To guarantee the experimental data quality in this work, a double second test is described below.

(b) Hand[37] and Othmer−Tobias[38] correlations, eqs 8 and 9, respectively, are used for low solute concentrations and low mutual solubility between solvents.

$$\log\left(\frac{x_2^{ilp}}{x_1^{ilp}}\right) = k_{1H}\log\left(\frac{x_2^{ap}}{x_3^{ap}}\right) + k_{2H} \quad (8)$$

$$\log\left(\frac{1-x_1^{ilp}}{x_1^{ilp}}\right) = k_{1OT}\log\left(\frac{1-x_3^{ap}}{x_3^{ap}}\right) + k_{2OT} \quad (9)$$

k_1 are the angular coefficients, while k_2 are the linear coefficients. The standard deviations for Hand and

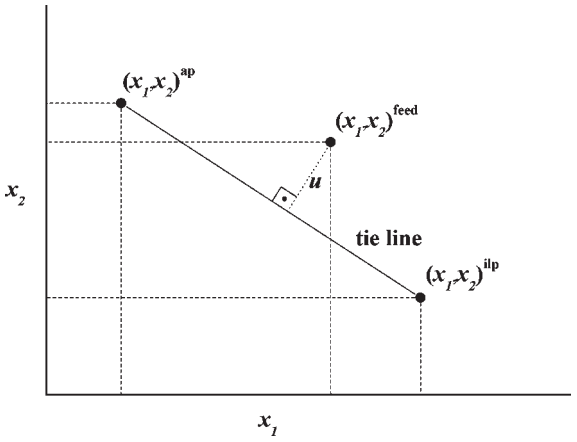

Figure 7. Geometric scheme for calculation of the distance (u) between the feed point and the tie line.

Table 6. Hand and Othmer−Tobias Coefficients k_1 and k_2, Correlation Coefficient R^2, and Standard Deviations σ for Systems Studied in This Work

	Hand				Othmer−Tobias			
T/K	k_{1H}	k_{2H}	R^2	σ	k_{1OT}	k_{2OT}	R^2	σ
[emim][DEtPO$_4$] (1) + 4,6-DMDBT (2) + n-Dodecane (3)								
298.2	1.5293	0.5946	0.9878	0.0529	0.1656	−1.7614	0.9900	0.0051
313.2	1.7121	1.1427	0.9999	0.0020	1.0974	0.4032	0.9817	0.0228
[emim][EtSO$_4$] (1) + 4,6-DMDBT (2) + n-Dodecane (3)								
298.2	1.3687	−0.2867	0.9977	0.0262	0.1416	−2.1133	0.9655	0.0108
313.2	0.5701	−0.3339	0.9996	0.0042	0.2956	−1.6336	0.9923	0.0051

Othmer−Tobias (σ) were calculated with eq 10.

$$\sigma = \sqrt{\frac{\sum_i^d (F_{exp} - F_{calc})_i^2}{d-q}} \quad (10)$$

where F_{exp} and F_{calc} represent the experimental and calculated left-hand side of eqs 8 and 9, and q is the number of coefficients of Hand or Othmer−Tobias equations.

Table 6 presents k_1, k_2, R^2, and σ calculated here. Figures 8 and 9 show Hand and Othmer−Tobias experimental data and their linear regression. The data quality is shown by a $R^2 > 0.98$ for [emim][DEtPO$_4$] and $R^2 > 0.96$ for [emim][EtSO$_4$] systems. Also, $\sigma < 0.053$ for Hand and $\sigma < 0.023$ for the Othmer−Tobias equation were achieved for all systems.

Removal of 4,6-DMDBT. The 4,6-DMDBT extraction percent (E) can be calculated by:

$$E = \frac{C_0 - C_f}{C_0} \cdot 100 \quad (11)$$

$$C_0 = \left(\frac{w_2}{w_2 + w_3}\right)_{feed} \quad (12)$$

$$C_f = \left(\frac{w_2}{w_2 + w_3}\right)_{alkane\ phase} \quad (13)$$

where C_0 and C_f are the mass fractions of 4,6-DMDBT in dodecane before and after equilibrium, respectively. The results

dx.doi.org/10.1021/je100991y |J. Chem. Eng. Data 2011, 56, 2005–2012

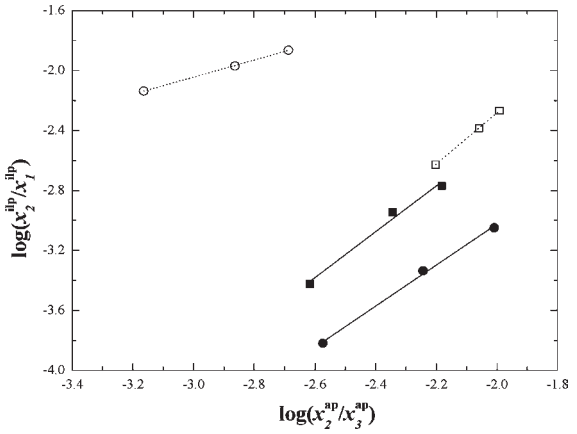

Figure 8. Hand correlation for LLE data: □, [emim][DEtPO$_4$]; ○, [emim][EtSO$_4$]; full symbols and solid lines, 298.2 K; open symbols and dotted lines, 313.2 K. Component numbers: ionic liquid (1), 4,6-DMDBT (2), dodecane (3).

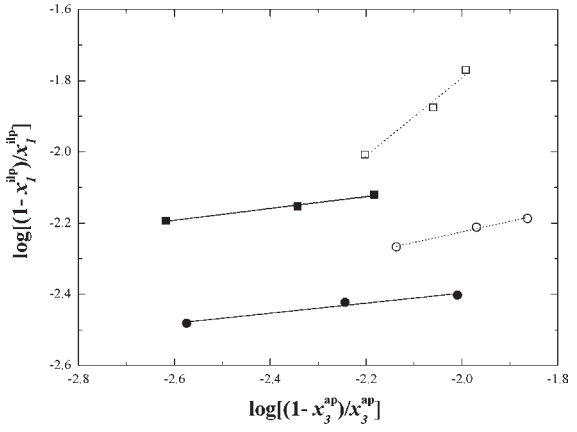

Figure 9. Othmer−Tobias correlation for LLE data: □, [emim][DEtPO$_4$]; ○, [emim][EtSO$_4$]; full symbols and solid lines, 298.2 K; open symbols and dotted lines, 313.2 K. Component numbers: ionic liquid (1), 4,6-DMDBT (2), dodecane (3).

for an ionic liquid/dodecane feed mass ratio = 0.6 are shown in Table 7 and Figure 10. For all systems, the percent of 4,6-DMDBT extraction was $E < 19$, and the best values were found with [emim][DEtPO$_4$]. An increase in temperature from 298.2 K to 313.2 K does not change significantly E for both ionic liquids.

Since the ionic liquids studied here are potential extractive desulfurization solvents, their regeneration is an important issue. Although it is beyond the scope of this work, some insights can be given. In literature,[39] supercritical carbon dioxide has been already tested to remove aromatic sulfur compounds from ionic liquid. The regeneration could be also investigated by mixing water with an ionic liquid-rich phase; water would solubilize a great amount of ionic liquid, which presents high hydrophylicity, 4,6-DMDBT would settle as a solid phase, and dodecane would form a liquid phase above the water phase. Analyzing the ionic liquid content on water phase would indicate the extent of regeneration. Filtration would remove the solid phase, and evaporation under vacuum would separate water from ionic liquid.

NRTL Parameters. The estimated nonrandom two-liquid (NRTL) parameters are given in Table 8, and the calculated tie lines are shown in Figures 1 to 4. The calculated solute distribution between both phases are in Figure 5. The deviations

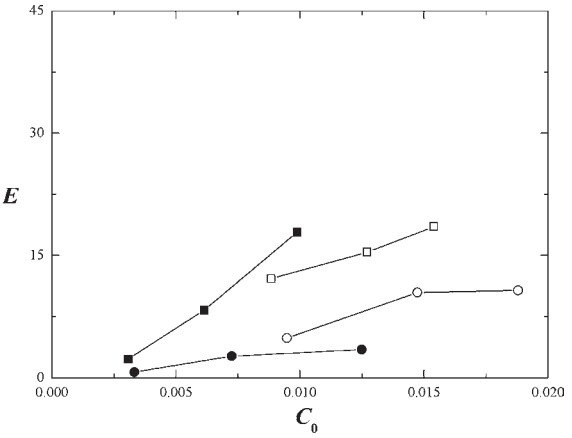

Figure 10. Extraction percent E of 4,6-DMDBT from dodecane for each mass fraction of 4,6-DMDBT before equilibrium C_0: □, emim]-[DEtPO$_4$]; ○, [emim][EtSO$_4$]; full symbols, 298.2 K; open symbols, 313.2 K. Ionic liquid/dodecane feed mass ratio = 0.6. Component numbers: ionic liquid (1), 4,6-DMDBT (2), dodecane (3).

Table 7. Extraction Percent E of 4,6-DMDBT from Dodecane by Ionic Liquids at 298.2 K and 313.2 K for Three Initial Concentrations[a]

T/K	[emim][DEtPO$_4$]		[emim][EtSO$_4$]	
	C_0	E	C_0	E
298.2	0.0031	2.3	0.0033	0.69
	0.0061	8.3	0.0073	2.67
	0.0099	17.9	0.0125	3.45
313.2	0.0088	12.17	0.0095	4.86
	0.0127	15.42	0.0147	10.46
	0.0154	18.55	0.0188	10.72

[a] Ionic liquid/dodecane feed mass ratio = 0.6.

Table 8. Estimated NRTL Parameters A, B, and α, Root-Mean-Square Deviations δx, and Objective Function F[a]

i	j	A_{ij}	A_{ji}	B_{ij}/K	B_{ji}/K	α_{ij}
[emim][DEtPO$_4$] (1) + 4,6-DMDBT (2) + Dodecane (3), δx = 0.0002; F = 0.33						
1	2	−2382.0	−641.5	14.8	−2.2	0.2
1	3	1564.7	7710.4	−1.2	−15.8	0.2
2	3	−5360.1	−249.5	17.0	−3.9	0.2
[emim][EtSO$_4$] (1) + 4,6-DMDBT (2) + Dodecane (3), δx = 0.0001; F = 0.07						
1	2	−428.2	3505.0	−8.2	−7.2	0.2
1	3	2047.4	−1029.4	−2.5	12.9	0.2
2	3	143.8	−2485.9	−3.6	3.7	0.2

[a] Note: δx values represent the root-mean-square deviations between experimental and NRTL calculated mole fractions; the F values represent the minimum calculated for objective function using the estimated parameters A, B, and α_{ij} for the systems studied.

dx.doi.org/10.1021/je100991y |J. Chem. Eng. Data 2011, 56, 2005–2012

between experimental and calculated compositions of both equilibrium phases were below $\delta x = 0.0002$.

CONCLUSIONS

Rectangular phase diagrams showing experimental phase equilibrium data were obtained for the {[emim][$DEtPO_4$] or [emim][$EtSO_4$]} + 4,6-DMDBT + dodecane systems at 298.2 K and 313.2 K and ≈ 95 kPa. The quality of the data was ascertained by the Hand and Othmer−Tobias correlations, with a $R^2 > 0.96$. Both ionic liquids did not dissolve in dodecane, but dodecane is present as small amounts in the ionic liquid-rich phase. It is observed, from values of solute distribution, solvent selectivity, and percent of removal, that [emim][$DEtPO_4$] is a better solvent than [emim][$EtSO_4$] for the extraction of 4,6-DMDBT from dodecane. A percent of extraction below 19 was achieved with both ionic liquids. The LLE data were correlated with the NRTL model, with the estimation of new energy interaction parameters. The deviations between experimental and calculated compositions were always below $\delta x = 0.0002$.

AUTHOR INFORMATION

Corresponding Author

*Tel.: +55 19 3521 3962. E-mail: maznar@feq.unicamp.br.

Funding Sources

Financial support from FAPESP (Grants 07/53024-3 and 07/52032-2) is gratefully acknowledged. M.A. is the recipient of a CNPq fellowship.

Notes

†E-mail: leonardoh.deoliveira@gmail.com.

REFERENCES

(1) Araújo, J. A.; Santos, F. K. G.; Barbosa, C. M. B. M.; Carvalho, M. W. N. C. *Desulfurization of cyclohexene-propanethiol fuel mixture by using ME/ALPO's type adsorbents*, 4th Brazilian Congress of Oil and Gas Research and Development, Campinas, Brazil, 2007.

(2) National Transport Comission. *Deployment Schedule for Cleaner Diesel, Environmental Program for Transportation − DESPOLUIR*. http://www.cntdespoluir.org.br (accessed Dec 8, 2009).

(3) Esser, J.; Wasserscheid, P.; Jess, A. Deep desulfurization of oil refinery streams by extraction with ionic liquids. *Green Chem.* **2004**, *6*, 316–322.

(4) Wasserscheid, P.; Bössmann, A.; Jess, A.; Datsevich, L.; Schmitz, C.; Wendt, A. Process for removing polar impurities from hydrocarbons and mixture of hydrocarbons. US Patent No. 2005/0010076 A1, January 13, 2005.

(5) Kwak, C.; Lee, J. J.; Bae, J. S.; Choi, K.; Moon, S. H. Hydrodesulfurization of DBT, 4-MDBT, and 4,6-DMDBT on fluorinated $CoMoS/Al_2O_3$ catalysts. *Appl. Catal., A* **2000**, *200*, 233–242.

(6) Sévignon, M.; Macaud, M.; Favre-Réguillon, A.; Schulz, J.; Rocault, M.; Faure, R.; Vrinat, M.; Lemaire, M. Ultra-deep desulfurization of transportation fuels via charge-transfer complexes under ambient conditions. *Green Chem.* **2005**, *7*, 413–420.

(7) Kabe, T.; Ishihara, A.; Tajima, H. Hydrodesulfurization of sulfur-containing polyaromatic compounds in light oil. *Ind. Eng. Chem. Res.* **1992**, *31*, 1577–1580.

(8) Kirimura, K.; Furuya, T.; Nishii, Y.; Ishii, Y.; Kino, K.; Usami, S. Biodesulfurization of dibenzothiophene and its derivatives through the selective cleavage of carbon-sulfur bonds by a moderately thermophilic bacterium *Bacillus subtilis* WU-S2B. *J. Biosci. Bioeng.* **2001**, *91*, 262–266.

(9) Mohebali, G.; Ball, A. S. Biocatalytic desulfurization (BDS) of petrodiesel fuels. *Microbiology* **2008**, *154*, 2169–2183.

(10) Isoda, T.; Nagao, S.; Ma, X.; Korai, Y.; Mochida, I. Hydrodesulfurization of refractory sulfur species. 2. Selective hydrodesulfurization of 4,6-dimethyldibenzothiophene in the dominant presence of naphthalene over ternary sulfides catalyst. *Energy Fuels* **1996**, *10*, 487–492.

(11) Landau, M. V.; Berger, D.; Herskowitz, M. Hydrodesulfurization of methyl-substituted dibenzothiophenes: fundamental study of routes to deep desulfurization. *J. Catal.* **1996**, *159*, 236–245.

(12) Te, M.; Fairbridge, C.; Ring, Z. Oxidation reactivities of dibenzothiophenes in polyoxometalate/H_2O_2 and formic acid/H_2O_2 systems. *Appl. Catal., A* **2001**, *219*, 267–280.

(13) Yazu, K.; Yamamoto, Y.; Furuya, T.; Miki, K.; Ukegawa, K. Oxidation of dibenzothiophenes in an organic biphasic system and its application to oxidative desulfurization of light oil. *Energy Fuels* **2001**, *15*, 1535–1536.

(14) Ma, X.; Sakanishi, K.; Mochida, I. Hydrodesulfurization reactivities of various sulfur compounds in diesel fuel. *Ind. Eng. Chem. Res.* **1994**, *33*, 218–222.

(15) Hernández-Maldonado, A. J.; Yang, R. T. Desulfurization of commercial liquid fuels by selective adsorption via π-complexation with Cu(I)-Y zeolite. *Ind. Eng. Chem. Res.* **2003**, *42*, 3103–3110.

(16) Zhang, S.; Zhang, Q.; Zhang, Z. C. Extractive desulfurization and denitrogenation of fuels using ionic liquids. *Ind. Eng. Chem. Res.* **2004**, *43*, 614–622.

(17) Qian, E. W. Development of novel nonhydrogenation desulfurization process − oxidative desulfurization of distillate. *J. Jpn. Petrol. Inst.* **2008**, *51* (1), 14–31.

(18) Lecrenay, E.; Sakanishi, K.; Nagamatsu, T.; Mochida, I.; Suzuka, T. Hydrodesulfurization activity of CoMo and NiMo supported on Al_2O_3-TiO_2 for some model compounds and gas oils. *Appl. Catal., B* **1998**, *18*, 325–330.

(19) Mochida, M.; Sakanishi, K.; Ma, X.; Nagao, S.; Isoda, T. Deep hydrodesulfurization of diesel fuel: design of reaction process and catalysts. *Catal. Today* **1996**, *29*, 185–189.

(20) Al-Shahrani, F.; Xiao, T.; Llewellyn, S. A.; Barri, S.; Jiang, Z.; Shi, H.; Martinie, G.; Green, M. L. H. Desulfurization of diesel via the H_2O_2 oxidation of aromatic sulfides to sulfones using a tungstate catalyst. *Appl. Catal., B* **2007**, *73*, 311–316.

(21) Bösmann, A.; Datsevich, L.; Jess, A.; Lauter, A.; Schmitz, C.; Wasserscheid, P. Deep desulfurization of diesel fuel by extraction with ionic liquids. *Chem. Commun.* **2001**, 2494–2495.

(22) Nie, Y.; Li, C.-X.; Wang, Z.-H. Extractive desulfurization of fuel oil using alkylimidazole and its mixture with dialkylphosphate ionic liquids. *Ind. Eng. Chem. Res.* **2007**, *46*, 5108–5112.

(23) Alonso, L.; Arce, A.; Francisco, M.; Soto, A. (Liquid + liquid) equilibria of [C_8mim][NTf_2] ionic liquid with a sulfur-component and hydrocarbons. *J. Chem. Thermodyn.* **2008**, *40*, 265–270.

(24) Alonso, L.; Arce, A.; Francisco, M.; Soto, A. Solvent extraction of thiophene from n-alkanes (C_7, C_{12}, and C_{16}) using the ionic liquid [C_8mim][BF_4]. *J. Chem. Thermodyn.* **2008**, *40*, 966–972.

(25) Alonso, L.; Arce, A.; Francisco, M.; Soto, A. Phase behaviour of 1-methyl-3-octylimidazolium bis[trifluoromethylsulfonyl]imide with thiophene and aliphatic hydrocarbons: The influence of n-alkane chain length. *Fluid Phase Equilib.* **2008**, *263*, 176–181.

(26) Alonso, L.; Arce, A.; Francisco, M.; Soto, A. Thiophene separation from aliphatic hydrocarbons using the 1-ethyl-3-methylimidazolium ethylsulfate ionic liquid. *Fluid Phase Equilib.* **2008**, *270*, 97–102.

(27) Oliveira, L. H.; Aznar, M. Liquid-liquid equilibrium data in ionic liquid + 4-methyldibenzothiophene + dodecane systems. *Ind. Eng. Chem. Res.* **2010**, *49*, 9462–9468.

(28) Wohlfarth, C. Refractive index of dodecane. *Landolt-Börnstein III/47: Optical Constants* **2008**, *47*, 528–530.

(29) Sandler, S. I. *Chemical, Biochemical, and Engineering Thermodynamics*; John Wiley & Sons: Hoboken, NJ, 2006.

(30) Oliveira, L. H. *Thermodynamic Study of Liquid-liquid Equilibrium aiming the Sulfur Removal from Diesel Oil Utilizing Ionic Liquids*. M.Sc. Dissertation, School of Chemical Engineering, University of Campinas, Campinas, 2009.

(31) Letcher, T. M.; Siswana, P. M. Liquid-liquid equilibria of mixtures of an alkanol + water + a methyl substituted benzene at 25 °C. *Fluid Phase Equilib.* **1992**, *74*, 203–217.

(32) Renon, H.; Prausnitz, J. M. Local compositions in thermodynamic excess functions for liquid mixtures. *AIChE J.* **1968**, *14*, 135–144.

(33) Stragevitch, L. *Liquid-liquid Equilibrium in Non-electrolyte Systems*. D.Sc. Thesis, School of Chemical Engineering, University of Campinas, Campinas, 1997.

(34) Nelder, J. A.; Mead, R. A Simplex method for function minimization. *Comput. J.* **1965**, *7*, 308–317.

(35) Sørensen, J. M.; Magnussen, T.; Rasmussen, P.; Fredenslund, A. Liquid-liquid equilibrium data: their retrieval, correlation and prediction. Part II: correlation. *Fluid Phase Equilib.* **1979**, *3*, 47–82.

(36) Anton, H.; Rorres, C. *Elementary Linear Algebra: Applications Version*, 9th ed.; Wiley: Hoboken, NJ, 2005.

(37) Hand, D. B. Dineric distribution. *J. Phys. Chem.* **1930**, *34*, 1961–2000.

(38) Othmer, D. F.; Tobias, P. E. Tie-line correlation. *Ind. Eng. Chem.* **1942**, *34*, 693–696.

(39) Planeta, J.; Karásek, P.; Roth, M. Distribution of sulfur-containing aromatics between [hmim][Tf_2N] and supercritical CO_2: a case study for deep desulfurization of oil refinery streams by extraction with ionic liquids. *Green Chem.* **2006**, *8*, 70–77.